5. Swope, H. H. *Harvard Obs. Bull.* **913,** 11-12 (1940).
6. Heathcote, S. R. & Suntzeff, N. B. *IAU Circ.* No. 4567 (1988).
7. Rosa, M. *Mercury* Vol. XVII, 63 (1988).
8. Phillips, M. M., Heathcote, S. R., Hamuy, M. & Navarrete, M. *Astron. J.* **95,** 1087-1110 (1988).
9. Hamuy, M., Suntzeff, N. B., Gonzalez, R. & Martin, G. *Astron. J.* **95,** 63-83 (1988).
10. Blanco, V. M. *et al. Astrophys. J.* **320,** 589-596 (1987).
11. Phillips, M. M. *Proc. George Mason Conf. on SN1987A* (eds Kafatos, M. & Michalitsianos, A. G.) (Cambridge University Press, London, 1988).
12. Hanuschik, R. W. & Dachs, J. *Astr. Astrophys.* **182,** L29-L30 (1987).
13. Couderc, P. *Annls d'Astrophys.* **2,** 271-302 (1939).
14. Chevalier, R. A. *Astrophys. J.* **308,** 225-231 (1986).
15. Schaefer, B. E. *Astrophys. J.* **323,** L47-L49 (1987).
16. Chevalier, R. A. *Proc. ESO Workshop on the SN1987A* (ed. Danziger, I. J.) 481-494 (ESO publications, Garching, 1987).
17. Katz, J. I. & Jackson, S. *Astr. Astrophys.* (in the press).
18. Magain, P. *Nature* **329,** 606-607 (1987).
19. Andreani, P., Ferlet, R. & Vidal-Madjar, A. *Nature* **326,** 770-772 (1987).
20. Freeman, K. C., Illingworth, G. & Oemler, A. Jr *Astrophys. J.* **272,** 488-508 (1983).
21. Freeman, K. C. in *Structure and Evolution of the Magellanic Clouds* IAU Symp. No. 108 (eds van den Bergh, S. & de Boer, K. S.) 107-114 (Reidel, Dordrecht, 1984).
22. Nisenson, P., Papaliolios, C., Karovska, M. & Noyes, R. *Astrophys. J.* **320,** L15-L18 (1987); *Erratum* **324,** L35 (1988).
23. Meikle, W. P. S., Matcher, S. J. & Morgan, B. L. *Nature* **329,** 608-611 (1987).
24. Hillebrandt, W., Hoflich, P., Schmidt, H. U. & Truran, J. W. *Astr. Astrophys.* **186,** L9-L10 (1987).
25. Rees, M. J. *Nature* **328,** 206 (1987).
26. Goldman, I. *Astr. Astrophys.* **186,** L3-L4 (1987).
27. Draine, B. T. *Astrophys., J. Suppl.* **57,** 587-594 (1985).

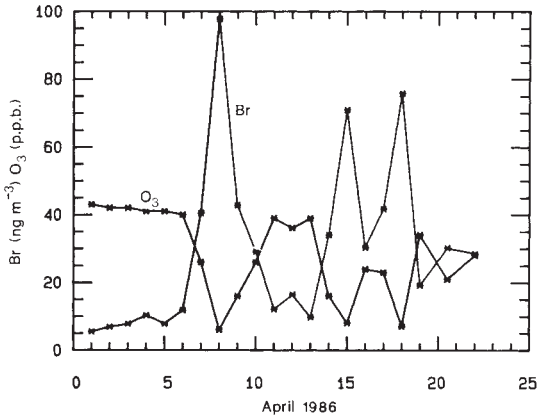

Fig. 1 A comparison of daily mean ground level O_3 and filterable Br(f-Br) concentrations at Alert, Canada, in April 1986 (from Barrie *et al.*[2]), illustrating the strong inverse correlation between the two parameters.

Ozone destruction and photochemical reactions at polar sunrise in the lower Arctic atmosphere

L. A. Barrie*, J. W. Bottenheim*, R. C. Schnell†, P. J. Crutzen‡ & R. A. Rasmussen§

* Atmospheric Environment Service, 4905 Dufferin Street, Downsview, Ontario, Canada M3H 5T4
† Cooperative Institute for Research in Environmental Sciences (CIRES), University of Colorado, Box 449, Boulder, Colorado 80309, USA
‡ Max Planck Institute for Chemistry, Postfach 3060, D-6500 Mainz, FRG and Department of Geophysical Sciences, University of Chicago, 5734 South Ellis Avenue, Chicago, Illinois 60637, USA
§ Institute of Atmospheric Sciences, Oregon Graduate Center, Beaverton, Oregon 97006, USA

There is increasing evidence that at polar sunrise sunlight-induced changes in the composition of the lower Arctic atmosphere (0–2 km) are taking place that are important regarding the tropospheric cycles of ozone, bromine, sulphur oxides[1], nitrogen oxides[2] and possibly iodine[3]. Here we focus on recent ground-level observations from the Canadian baseline station at Alert (82.5° N, 62.3° W) and from aircraft that show that ozone destruction is occurring under the Arctic surface radiation inversion during March and April as the Sun rises. The destruction might be linked to catalytic reactions of BrO_x radicals and the photochemistry of bromoform, which appears to have a biological origin in the Arctic Ocean. This may clarify previously unexplained regular springtime occurrences of ozone depletion at ground level in a 10-year data record at Barrow, Alaska[4], as well as peaks in aerosol bromine observed throughout the Arctic in March and April[3]. Current information does not allow us to offer more than a speculative explanation for the chemical mechanisms leading to these phenomena.

It has been found in recent years that the Arctic atmosphere is highly polluted during winter because of strong transport from Eurasia to the pole, weak pollutant removal by precipitation and inefficient uptake at the cold, relatively inert Earth's surface[5]. This pollution has been present since at least the turn of the century and has been on the increase from 1950 to 1980 owing to increasing industrial activity[6,7]. The phenomenon of visibility-reducing air pollution commonly known as 'Arctic haze' has prompted new measurements of atmospheric composition at high-latitude stations on a long-term basis and periodic intensive airborne research[8,9].

Sudden disappearances of O_3 in air at ground level at Alert were first noticed during an intensive study in March 1985 (ref. 10). Volume mixing ratios dropped from 30 to 40 parts per billion (p.p.b.(v.)) to almost 0 p.p.b.(v.) in the time span of a few hours to a day. A more detailed field study during April 1986 confirmed that this was a regular occurrence at this time of year and that a chemical link with bromine existed. The latter was suggested by a strong anti-correlation between daily mean concentrations of O_3 and Br collected on cellulose Whatman 41 filters[2] (Fig. 1). We have reason to believe that the latter (which will henceforth be referred to as f-Br) is the sum of particulate Br and gaseous HBr. There are indeed indications from measurements at Alert that 50–93% of f-Br is gaseous, probably HBr (ref. 2).

Continuous ground-level O_3 records at Alert between February and June in 1986 and 1987 (Fig. 2) show that, while proceeding from dark winter to sunlit spring, sudden downward departures from the mean concentration curve occurred. The magnitude of the departure paralleled the increase of sunlight at polar sunrise. These data, when combined with observations from a routine weekly aerosol chemistry record at Alert, show that ozone was strongly anti-correlated with f-Br, even when averaged on a weekly basis.

Further evidence that the period of polar sunrise is marked by large variations in lower tropospheric O_3, and that the observations at Alert are typical of the lower Arctic atmosphere, is offered by 10 years of ground-level O_3 observations at Barrow, Alaska[4]. After polar sunrise in March and April as sunlight increases, not only is there a minimum in the median O_3 concentration observed, but also an absolute maximum in its variability.

Another piece of the puzzle was provided by aircraft observations over the Arctic icecap made during the spring months of March and April[11-13]. Whenever there was a strong surface radiation inversion, O_3 was depleted below the inversion, whereas fine particle mass was not. In addition, f-Br peaked in the near-surface layer[14,15].

The seasonal cycle of f-Br in the Arctic atmosphere has long been a curiosity[3,16,17]. Excess f-Br over that from windblown dust, sea salt and automobile fuel additives peaks in concentration in the spring months of March and April throughout the North American Arctic. The maximum, which occurs shortly after Arctic sunrise between late March and the end of April, has been tentatively attributed to photochemically induced conversion of gaseous organobromine compounds. The average

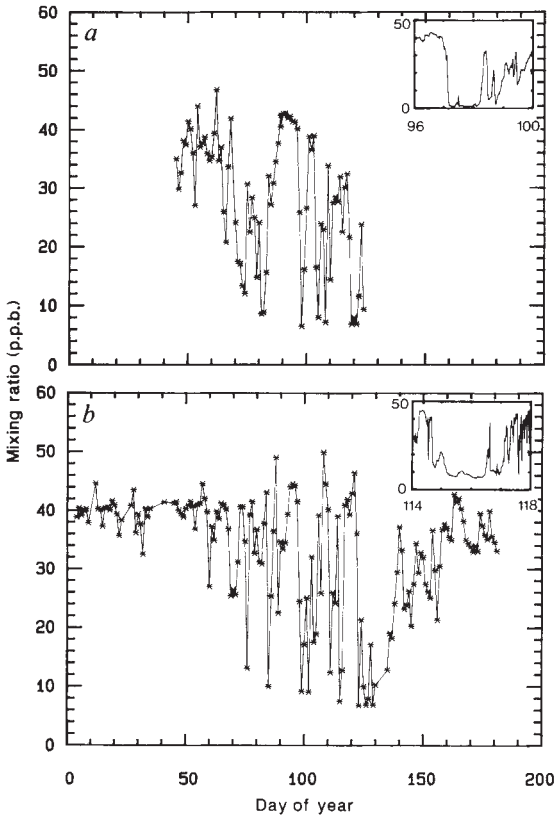

Fig. 2 Daily average concentrations of O_3 observed at ground level at Alert in the Canadian high Arctic during the first half of *a*, 1986 and *b*, 1987 (J.W.B.). Note the dip in concentration and the greater variability following polar sunrise, which occurs in early March. The inserted figures show examples of continuous measurements during selected low-O_3 episodes.

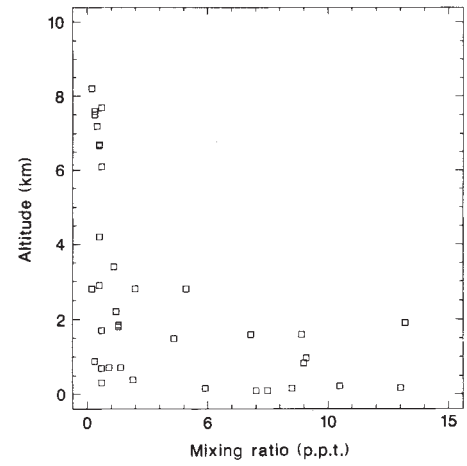

Fig. 3 The vertical distribution of bromoform concentrations in the Arctic atmosphere over the icecap during April 1986 reconstructed from flask measurements from aircraft (R.A.R.).

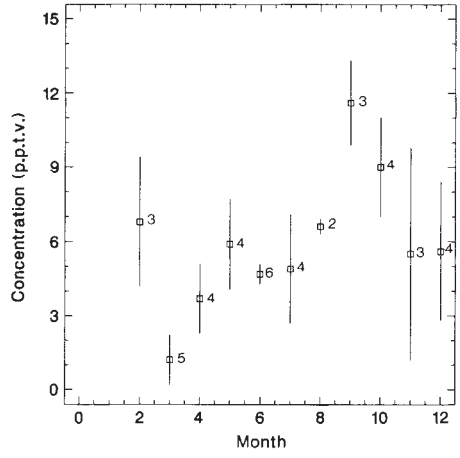

Fig. 4 The seasonal variation of ground level bromoform ($CHBr_3$) mixing ratio at Alert in the Canadian high Arctic obtained from routine weekly flask sample measurements in 1986 and 1987 (R.A.R.). Points on the graph are coded with the number of samples available.

concentration of the possible gaseous precursors of f-Br has been estimated for the Arctic and Antarctic lower troposphere by Khalil *et al.* from observations[18]. Total alkanobromine concentrations were found to be a factor of 3.6 higher in the Arctic than in Antarctica. Moreover, in contrast to the south polar region, the north has most of its alkanobromine as bromoform (57% versus 15%). This compound ($CHBr_3$) is the most easily photolysed of all the alkanobromine gases. Aircraft observations made in March 1983 suggest that its concentration peaks in the Arctic troposphere below the radiation inversion[19,20]. More extensive observations during April 1986 confirmed this (Fig. 3), which indicates that bromoform is being produced in the Arctic Ocean, possibly by decay of marine algae such as red benthic algae[21]. The seasonal variation of $CHBr_3$ at Alert during 1986 and 1987 is shown in Fig. 4. The seasonal variation of $CHBr_3$ is somewhat different from the pattern observed at Barrow, Alaska from 1984 to 1987 (ref. 22), but as a result of the limited number of samples per month (3–6 at Alert, 8 at Barrow), it is too early to judge whether these differences are significant. The fact remains that the most rapid decrease in bromoform is observed during polar sunrise. This is suggestive of photochemical activity of this gas.

In what follows, we propose an explanation for the observed depletion of O_3 and associated production of f-Br at polar sunrise in the lower Arctic troposphere. The scenario is as follows. Persistently throughout winter and early spring, the surface boundary layer of the Arctic troposphere over the icecap is isolated from the free tropospheric reservoir of O_3 by a strong radiation inversion. Ozone destruction and f-Br production from gaseous alkanobromines, principally $CHBr_3$, are induced in the boundary layer by sunlight at polar sunrise. The strong inversion inhibits the replenishment of O_3 from aloft and the dilution of f-Br produced. It also acts to trap organobromines generated by natural sources in the Arctic ocean and thereby enhances the rate of O_3 destruction and f-Br production. At Alert, what we are observing at ground level is the alternating presence of below-inversion air off the icecap and of above-inversion air mixed to the surface in winds coming off the rougher terrain of Ellesemere Island. The former is depleted in O_3 but enriched in f-Br, and in the latter the opposite occurs.

In theory, depletion of O_3 by dry deposition (namely, destruction at the Earth's surface) is possible. But observed dry-deposition velocities of O_3 to snow surfaces[23] are low (0.0006 m s^{-1}). Thus, the time to deplete 90% of ozone from a 1,000 m layer (a typical height for the surface radiation inversion) is about 44 days. This is much longer than the average transit time of an air parcel across the Arctic[24]. Hence dry deposition appears to be an insufficient sink for surface O_3. In addition, dry deposition as the main loss mechanism of O_3 does not explain why low O_3 concentrations are not observed during the dark winter.

We favour a chemical explanation (see Table 1), in which ozone destruction occurs by the catalytic cycle of reactions R2, followed by reactions R3*a* or R3*b* (Br_2 very rapidly photolyses

Table 1 Chemical reactions postulated to be involved in ozone destruction during polar sunrise involving ozone active bromine and NO_x catalysts

Reaction	Rate coefficient		
$CHBr_3 + h\nu$	$\rightarrow Br + CHBr_2$	$J_1 = 6\times10^{-7}$,	(R1)
	$\rightarrow n.\ BrO_x$	$n = 1, 2$ or 3	
$Br + O_3$	$\rightarrow BrO + O_2$	$k_2 = 7\times10^{-13}$	(R2)
$BrO + BrO$	$\rightarrow 2\ Br + O_2$	$k_{3a} = 2.5\times10^{-12}$	(R3*a*)
	$\rightarrow Br_2 + O_2 + (h\nu)$	$k_{3b} = 7\times10^{-13}$	(R3*b*)
	$\rightarrow 2\ Br + O_2$		
$BrO + NO$	$\rightarrow Br + NO_2$	$k_4 = 2.5\times10^{-11}$	(R4)
$BrO + h\nu$	$\rightarrow Br + O$	$J_5 = 5\times10^{-3}$	(R5)
$NO_2 + h\nu$	$\rightarrow NO + O$	$J_6 = 2.5\times10^{-3}$	(R6)
$O + O_2\ (+M)$	$\rightarrow O_3\ (+M)$	$k_7 = 2\times10^{-14}$	(R7)
$NO + O_3$	$\rightarrow NO_2 + O_2$	$k_8 = 7\times10^{-15}$	(R8)
$BrO + NO_2\ (+M)$	$\rightarrow BrONO_2\ (+M)$	$k_9 = 2\times10^{-11}$	(R9)
$BrONO_2 + h\nu$	$\rightarrow BrO + NO_2\ (?)$	$J_{10} = 4\times10^{-4}$	(R10)
$Br + CH_2O$	$\rightarrow HBr + CHO$	$k_{11a} = 7\times10^{-13}$	(R11*a*)
$Br + HO_2$	$\rightarrow HBr + O_2$	$k_{11b} = 8\times10^{-13}$	(R11*b*)
$CH_2O + h\nu$	$\rightarrow CO + H_2$	$J_{12a} = 1.5\times10^{-5}$	(R12*a*)
	$\rightarrow H + CHO + (2O_2)$	$J_{12b} = 6.5\times10^{-6}$	(R12*b*)
	$\rightarrow 2HO_2$		
$O_3 + h\nu$	$\rightarrow O(^1D) + O_2$	$J_{13} = 7\times10^{-7}$	(R13)
$O(^1D) + H_2O$	$\rightarrow 2OH$	$k_{14} = 2.3\times10^{-10}$	(R14)
$HBr + OH$	$\rightarrow Br + H_2O$	$k_{15} = 1.0\times10^{-11}$	(R15)
$BrO + HO_2$	$\rightarrow BrOH + O_2 + (h\nu)$	$k_{16} = 5.0\times10^{-12}$	(R16)
	$\rightarrow Br + OH$		

All rate constants, in units of s^{-1} and $cm^3\ molec^{-1}\ s^{-1}$, are estimated for the environmental conditions during the measurement period (250 K, one atmosphere pressure) from data in ref. 29. Other reactions involving HO_x, CH_4, CO, and their reactive products are standard. *J*-values are arithmetic averages, in time, diurnally for a three-week period centred on 1 April and, in space, for latitudes 65, 75 and 85° N, calculated with a multiple scattering routine for 400 overhead Dobson units and for average cloudiness conditions.

into two Br atoms). This cycle is moderated by NO_x ($NO + NO_2$) as a result of reactions R4 and R5, which negate ozone loss by the reformation of ozone through reactions R6 and R7. Similarly, the formation of $BrONO_2$ in reaction R9 decreases ozone destruction by removing BrO. Reaction R11*a* of Br with CH_2O also reduces the efficiency of O_3 destruction, but concentrations of CH_2O during early springtime in the Arctic should be low as a result of relatively rapid photolysis (reactions R12*a* and *b*). Furthermore, production of CH_2O due to methane oxidation (not shown in Table 1) is inefficient at this time of year because of the low rate of OH production by reactions R13 and R14. We calculate typical CH_2O mixing ratios in the 10–30 parts per trillion (p.p.t.(v.)) range. Preliminary results at Alert in March–April 1988 show that CH_2O and NO_x concentrations are low (<50 p.p.t.(v.)). The Arctic conditions in the lower troposphere may, therefore, correspond to those in the 'ozone hole' of the Antarctic lower stratosphere, which likewise are characterized by low NO_x concentrations[25,26].

There are two potential sources of BrO_x: reaction R1 (the photolysis of bromoform) or reaction between OH and HBr (R15). Recent independent measurements of the absorption cross-sections of $CHBr_3$ by S. Penkett and R. A. Cox (Harwell, UK) and by W. Schneider and G. Moortgat (Mainz, FRG), and detailed radiative transfer calculations for typical conditions on 1 April indicate an average diurnal photolysis rate constant of $6\times10^{-7}\ s^{-1}$ north of 65° N. Photolysis leads directly to the formation of one Br atom; subsequent oxidation reactions of the $CHBr_2$ fragment, probably by CBr_2O photolysis, may produce two additional BrO_x (Br + BrO) radicals.

Selected results of model simulations for the spring period using the reactions outlined in Table 1 are shown in Table 2. The right-hand column is the per cent change in ozone after three weeks. A constant volume mixing ratio of $CHBr_3$ of about 8 p.p.t.(v.) was used. This is consistent with aircraft observations over the icecap in Fig. 4. Ozone depletion depends on the amount of HBr and, for concentrations greater than a value in the 10–100 p.p.t.(v.) range, on that of NO_x. In the case of the f-Br captured by the filter being representative of gaseous HBr (~30 p.p.t.(v.) HBr), our model predicts 50–60% ozone destruction for 1–10 p.p.t.(v.) NO_x over an integration time of three weeks centred on April. In contrast, for the same NO_x range but in the absence of HBr, 20–25% O_3 destruction is predicted.

Table 2 Results of model calculations simulating chemical reactions in the lower Arctic atmosphere during the period 21 March to 11 April

NO_x (p.p.t.(v.))	HBr (p.p.t.(v.))	BrO (p.p.t.(v.))	Br ($n\ cm^{-3}$)	OH ($n\ cm^{-3}$)	O_3 (p.p.b.(v.))	Per cent change in O_3
1	30	11	3.4×10^6	7.1×10^4	16	−60
10	30	9.6	3.3×10^6	7.8×10^4	19.2	−52
100	30	6.1	1.9×10^6	1.7×10^5	36.3	−9
1	0	5.6	1.5×10^6	7.5×10^4	30	−25
10	0	4.4	1.2×10^6	9.3×10^4	32	−20
100	0	1.0	3.7×10^5	9.0×10^4	45	+12.5

Only those results for initial volume mixing ratios of 40 p.p.b.(v.) of O_3, 100 p.p.t.(v.) of CH_2O and three weeks of computation are shown. All units are for volume mixing ratios, with the exception of those for Br and OH, which are given in molecules per cm^3. $CHBr_3$ was kept constant at 8 p.p.t.(v.) whereas HBr was either 0 or 30 p.p.t.(v.) and NO_x either 1, 10 or 100 p.p.t.(v.) It is assumed that three BrO_x molecules are produced for each $CHBr_3$ molecule photolysed. For BrO and OH, maximum values during the integration period are given. Volume mixing ratios for CH_4 and CO were held constant at 1,700 and 150 p.p.b.(v.) respectively. Note the possibility of relatively high Br atom concentrations approaching 10^7 per cm^3.

The main problem with the assumption of high gaseous HBr concentrations is its source in the atmosphere. If it came solely from $CHBr_3$ photolysis, a production time of about one month would be required, assuming a maximum possible production of three HBr molecules for each $CHBr_3$ molecule destroyed. Furthermore, conversion of BrO_x to HBr would be rather inefficient for low CH_2O concentrations. Thus, there may well be other sources of HBr. Altogether, it is clear that there are significant uncertainties that make our explanation of ozone destruction in the lower Arctic atmosphere very tentative, and emphasize the need for more diagnostic measurements. In view of the very efficient O_3 depletion that was observed and which we have considerable difficulty in modelling, it may be asked whether heterogeneous reactions on ice crystals could enhance BrO_x production and catalytic ozone destruction, in the way that probably occurs for ClO_x in the Antarctic lower stratosphere during springtime[27,28].

The proposed chemical mechanism implicitly excludes Cl-induced destruction of O_3, which makes the ozone loss distinct from the chemistry that has been postulated to create the 'ozone-hole' during the austral spring in the Antarctic lower stratosphere. In contrast to brominated or iodinated hydrocarbons, chloroform and other chlorinated hydrocarbons do not absorb solar radiation in the lower troposphere, and hence no Cl formation is possible by that route. Furthermore, the modelled ratio of ClO_x to HCl is much lower than the ratio of BrO_x to HBr. This is due to a reaction rate of OH with HCl that is 100-fold lower than with HBr(R15), and to the fact that the reaction of CH_4 with Cl atoms is exothermic whereas that with Br atoms is endothermic.

In conclusion, we would like to re-emphasize that more measurements are needed in the Arctic atmosphere during polar sunrise to elucidate the mechanism of ozone destruction. The Arctic atmosphere is a unique laboratory in which to study the chemical behaviour of anthropogenic and natural substances in the presence and absence of light. There is much to be learned from studies on this part of the globe about the biogeochemical cycles of ozone, nitrogen and sulphur oxides, as well as the cycles of the halogens Br and I.

Received 11 January; accepted 31 May 1988.

1. Barrie, L. A. & Hoff, R. M. *Atmos. Envir.* **18,** 2711–2722 (1984).
2. Barrie, L. A., den Hartog, G., Bottenheim, J. W. & Landsberger, S. *J. atmos. Chem.* (in the press).
3. Sturges, W. T. & Barrie, L. A. *Atmos. Envir.* **22,** 1179–1194 (1988).
4. Oltmans, S. J. & Komhyr, W. D. *J. geophys. Res.* **91,** 5229–5236 (1986).
5. Barrie, L. A. *Atmos. Envir.* **20,** 643–663 (1986).

6. Koerner, R. M. & Fisher, D. *Nature* **295,** 137-140 (1982).
7. Barrie, L. A., Fisher, D. & Koerner, R. M. *Atmos. Envir.* **19,** 2055-2063 (1985).
8. Schnell, R. C. *Geophys. Res. Lett.* **11,** 361-364 (1983).
9. Schnell, R. C., Watson, T. B. & Bodhaine, B. A. *J. atmos. Chem.* (in the press).
10. Bottenheim, J. W., Gallant, A. G. & Brice, K. A. *Geophys. Res. Lett.* **13,** 113-116 (1986).
11. Leaitch, W. R., Hoff, R. M. & MacPherson, J. I. *J. atmos. Chem.* (in the press).
12. Bridgman, H. A., Schnell, R. C., Herbert, G. A., Bodhaine, B. A. & Oltmans, S. J. *J. atmos. Chem.* (in the press).
13. Herbert, G. A. *et al. J. atmos. Chem.* (in the press).
14. Hansen, A. D. A. & Rosen, H. *Geophys. Res. Lett.* **11,** 381-384 (1984).
15. Sheridan, P. J. thesis, Univ. Maryland (1986).
16. Berg, W. W., Sperry, P. D., Rahn, R. A. & Gladney, E. S. *J. geophys. Res.* **88,** 6719-6736 (1983).
17. Barrie, L. A. *J. atmos. Chem.* **3,** 139-152 (1985).
18. Khalil, M. A. K., Rasmussen, R. A. & Gunawardena, R. *NOAA/GMCC Ann. Rep.* Vol. 15 (1986).
19. Rasmussen, R. A. & Khalil, M. A. K. *Geophys. res. Lett.* **11,** 433-436 (1984).
20. Berg, W. W. *et al. Geophys. res. Lett.* **11,** 429-432 (1984).
21. Dryssen, D. & Fogelqvist, E. *Oceanologica Acta* **4,** 313-317 (1981).
22. Cicerone, R. J., Heidt, L. E. & Pollock, W. H. *J. geophys. Res.* **93,** 3745-3750 (1988).
23. Galbally, I. E. & Roy, C. R. *Q. Jl R. met. Soc.* **106,** 599-620 (1980).
24. Patterson, D. E. & Husar, R. B. *Atmos. Envir.* **15,** 1479-1482 (1981).
25. Toon, O. B., Hamill, P., Turro, R. P. & Pinto, J. *Geophys. Res. Lett.* **13,** 1284-1287 (1986).
26. Crutzen, P. J. & Arnold, F. *Nature* **324,** 651-655 (1986).
27. Molina, M. J., Tso, T. L., Molina, L. T. & Wang, F. C-Y. *Science* **238,** 1253-1257 (1987).
28. Tolbert, M. A., Rossi, M. J., Malhotra, R. & Golden, D. M. *Science* **238,** 1258-1260 (1987).
29. *JPL/NASA* Publn Number 85-37 (Jet Propulsion Laboratory, Pasadena, California 1985).

Crystal structure of the 80 K superconductor $YBa_2Cu_4O_8$

P. Marsh, R. M. Fleming, M. L. Mandich, A. M. DeSantolo, J. Kwo, M. Hong & L. J. Martinez-Miranda*

AT&T Bell Laboratories, Murray Hill, New Jersey 07974, USA
* Department of Electrical Engineering, University of Pennsylvania, Philadelphia, Pennsylvania 19104, USA

Recently a new Y–Ba–Cu–O superconducting oxide has been prepared as a distinct phase in thin films[1–3]. The new phase was first seen as a defect structure in bulk samples of $YBa_2Cu_3O_7$ (refs 4–7) and found to contain an additional copper layer[7]. The proposed defect structure has a *c*-axis spacing of ~27 Å and a cation ratio of YBa_2Cu_4. Y–Ba–Cu–O films containing a majority phase with a 27 Å unit cell have been proposed as evidence of a distinct phase with the same structure as the defects (ref. 1 and K. Char *et al.*, unpublished results). Films of the new phase superconduct with a transition temperature of 80 K (K. Char *et al.*, unpublished results and refs 2 and 3). We show by X-ray crystallography of a film containing 85% of the new phase that the stoichiometry can be written as $YBa_2Cu_4O_8$. The new structure differs from $YBa_2Cu_3O_7$ in that the single, linear Cu–O chain parallel to the *b*-axis has been replaced by a double Cu–O chain with edge-sharing, square-planar oxygen coordination.

Zandbergen *et al.*[7] analysed the planar defects in $YBa_2Cu_3O_7$ by high-resolution electron microscopy and reported a defect consisting of a "CuO double-layer intercalation". A structure with a tetragonal symmetry was suggested where the additional copper layer is shifted by half-a-lattice spacing along the *a*-axis and the *b*-axis. Marshall *et al.*[1] prepared a film of nominal metal composition $Y_{1.4}Ba_{2.2}Cu_4$, the majority phase of which had a unit cell with a *c*-axis spacing of 27.2 Å, and so was postulated to be a distinct phase with the same structure as the planar defects seen earlier[4–7]. The films were shown to have an orthorhombic *A*-centred cell and a modification of the defect structure with orthorhombic *Ammm* symmetry was proposed (ref. 1 and K. Char *et al.*, unpublished results). In the orthorhombic model the extra copper cation is displaced along the *b*-axis only, rather than along both the *a*- and *b*-axes. None of the previous studies reports measurements of the oxygen stoichiometry of the new phase.

Here we measure the structure and composition of the new phase, $YBa_2Cu_4O_8$, by X-ray diffraction from a film. Films were prepared by pulsed excimer laser evaporation of a composite target containing BaF_2–Y_2O_3–CuO, as described earlier[3]. Films were grown on a {100} face of $SrTiO_3$ and found to be oriented with the *c*-axis of the film normal to the substrate. The film used in this study had a thickness of 6,000 ± 500 Å and a second-phase contamination of $YBa_2Cu_3O_7$ of 15%. Resistance measurements indicated an onset of superconductivity at 82 K, a zero resistance at 77 K, and a width (10-90%) of 3 K (ref. 3). The film *a* and *b* lattice parameters are about equal, with a value of 3.86 Å (as compared with 3.905 Å for $SrTiO_3$). The *c*-axis of the film is 27.24 Å, a value close to 7*c* of $SrTiO_3$. The observed selection rules produced diffraction with $l = 2n + 1$ absent if *h* and *k* were even, and $l = 2n$ absent if *h* and *k* were odd, and are not consistent with any tetragonal space group. We interpret the selection rules as evidence of diffraction from individual orthorhombic *A*-centred domains rotated by 90° about the *c*-axis. Such domains with a lateral extent of ~100 μm have been observed before[1,3]. Although the presence of oriented domains on a substrate do not necessarily imply twinning in the crystallographic sense, we will use conventional analysis of diffraction from a twinned crystal in the discussion that follows.

Because $YBa_2Cu_4O_8$ is only available as a distinct phase in films, a determination of the structure involves problems not encountered with bulk materials. The primary problem is a small data set containing no Friedel pairs. Additional data were collected using both Mo and Cu Kα radiation from a rotating anode source (repeated observations with Mo radiation provide further structural information because of anomalous dispersion.) The film was mounted on a four-circle diffractometer with Bragg-

Table 1 Measured and calculated F^2 for $YBa_2Cu_4O_8$

h	*k*	*l*	F_o^2	F_c^2
Mo radiation				
0	0	4	976	991
0	0	6	294	245
0	0	8	1,011	974
0	0	10	2,790	2,794
0	0	12	8,698	8,814
0	0	16	2,688	2,931
0	0	22	1,194	1,125
0	0	26	2,793	2,010
0	0	30	497	305
0	0	32	111	78
Cu radiation				
0	0	2	926	1,768
0	0	4	3,729	3,629
0	0	6	2,283	1,674
0	0	8	6,296	5,505
0	0	10	9,459	7,974
0	0	12	23,775	24,427
0	0	16	8,284	9,826
0	0	18	624	774
0	0	20	259	228
1	0	2	831	3,570
1	0	3	1,048	1,939
1	0	4	9,795	10,641
1	0	6	14,888	15,403
1	0	8	36,378	35,259
1	0	9	7,717	6,603
1	0	10	883	262
1	0	11	543	372
1	0	12	403	191
1	0	15	2,477	4,010
1	0	16	3,811	3,801
1	0	18	2,993	4,520
1	0	19	3,443	4,356
1	1	3	11,919	14,495
1	1	5	1,215	134
1	1	9	8,584	6,353
1	1	11	12,931	12,088
1	1	13	5,418	5,808
1	1	15	30,868	30,305
0	1	8	41,235	40,955